DFIG Based Wind Energy Conversion System using Back to Back Power Electronic Interface

LATA GIDWANI
Department of Electrical Engineering
Rajasthan Technical University
Rawatbhata Road, Kota, Rajasthan
INDIA
lata_gidwani@rediffmail.com

Abstract: - This paper presents a grid connected DFIG WECS using back to back power electronic interface. Transient simulations are carried out under the condition of sudden short circuit disturbances. The paper aims to present in a thorough and coherent way the aspects of power quality in terms of Total Harmonic Distortion (THD) at various fault locations and buses. Simulated results are obtained in detail. All the simulations are made in Matlab/Simulink.

Key-Words: - Doubly Fed Induction Generator, Power Electronic Interface, Power Quality, Total Harmonic Distortion, Wind Energy Conversion System.

1 Introduction

Wind Energy Conversion Systems (WECS) constitute a mainstream power technology that is largely under exploited. Wind technology has made major progression from the prototypes of just 30 years ago. The main differences in WECS technology are in electrical design and control. At present, typically two types of WECS for large wind turbines exists [1-3]. The first one is a variable speed WECS that allows variable speed operation over a large, but still restricted, range. This type of WECS mainly uses a Doubly Fed Induction Generator (DFIG) with the stator windings connected directly to the three phase constant – frequency grid and the rotor windings connected to a partial scale back to back converter. A multi stage gear box is necessary in this drive. This type of WECS offer high controllability, smoother grid connection, maximum power extraction and reactive power compensation using back to back power converters of rating near to 25-30% of the generator capacity [2-4]. The complete modelling and simulation of a grid interfaced WECS based on DFIG, using dynamic vector approach is presented in [7-8].

The paper is organized as follows: Section 1 presents an introduction along with objectives of the present work. System configuration and proposed strategy are described in Section 2. The simulation models developed in MATLAB Simulink are detailed in Section 3 and the results obtained from models are explained in Section 4. The conclusions drawn from these results are finally summarized in Section 5.

2 Modeling of Wind Turbine

The modelling of wind turbine will now be discussed here. The mechanical power available from a wind turbine is as follows [9] :

$$P_w = 0.5\ \rho\pi\ R^2\ V_w{}^3\ C_p(\lambda,\beta) \qquad (1)$$

where, P_w is power extracted from the wind, ρ is air density, R is blade radius, V_w is wind speed and C_p is power coefficient. C_p is given as a nonlinear function of the parameters tip speed ratio λ and blade pitch angle β. The calculation of the power coefficient requires the use of blade element theory. As this requires knowledge of aerodynamics and the computations are rather complicated, numerical approximations have been developed [10]. Here the following function will be used [9]

$$C_p = \frac{1}{2} * \left(\lambda - 0.022 * \beta^2 - 5.6\right) * e^{-0.17\lambda} \qquad (2)$$

where, λ is tip speed ratio and β is blade pitch angle. The tip speed ratio is given as :

$$\lambda = \frac{V_w}{\omega_B} \qquad (3)$$

where, ω_B is rotational speed of turbine. Usually C_p is approximated as,

$$C_p = \alpha\lambda + \beta\lambda^2 + \gamma\lambda^3 \quad (4)$$

where α, β and γ are constructive parameters for a given turbine. The torque developed by the windmill is

$$T_t = 0.5\,\rho\left(\frac{C_p}{\lambda}\right) V_w{}^3 \pi R^2 \quad (5)$$

To describe the impact of the dynamic behaviour of the wind turbine, a simple model is considered, where the tower bending mode and the flap-bending mode of the wind turbine are neglected [9]. Emphasis is placed on the parts of the dynamic structure of the wind turbine. The transmission is described by following equations :

$$I_{rot}\frac{d\omega_{rot}}{dt} = T_{rot} - T_{lss} \quad (6)$$

$$\frac{dT_{lss}}{dt} = k_s\left(\omega_{rot} - \frac{\omega_{gen}}{\eta_{gear}}\right) \quad (7)$$

where, I_{rot} is rotor inertia, ω_{rot} is turbine rotor speed, ω_{gen} is generator speed, T_{rot} is rotor torque, T_{lss} is low-speed shaft torque, k_s is shaft stiffness and η_{gear} is ratio of gear box. It is also assumed that the losses in the gearbox are zero. Thus the gear transmits ideally from the low speed to high speed. The output of the model is

$$T_{hss} = \frac{T_{lss}}{\eta_{gear}} \quad (8)$$

where, T_{hss} is high-speed shaft torque. The high speed shaft torque, T_{hss} is the mechanical torque input, T_m to wind generator used. The design parameters of wind turbine are shown in Table 1.

Table 1: Design Parameters of Wind Turbine

Wind Turbine Data for One Wind Turbine	
Nominal Wind Turbine Mechanical Power	3 x 10^6 Watt
Base Wind Speed	9 m/sec.
Pitch Angle Controller Proportional Gain	5
Pitch Angle Controller Integral Gain	25
Maximum Pitch Angle	45 deg.
Maximum Rate of Change of Pitch Angle	2 deg./sec

3 WECS using DFIG with Back to Back Converters

This section considers the mutual effects of integrating wind power using DFIG with back to back converters in power systems under transient fault situations. A 9 MW wind-farm consisting of three 3 MW wind turbines, connected to a 33 kV distribution system, exports power to a 220 kV grid through a 30 km, 33 kV feeder. A 500 KW resistive load and a 0.9 MVAR (Q = 50) filter are connected at the 440 V bus. A fault is simulated and connected to 132 kV line and grounding transformer is connected to 33 kV bus. Fig.1 shows the layout of the wind system with its interconnection to the transmission grid.

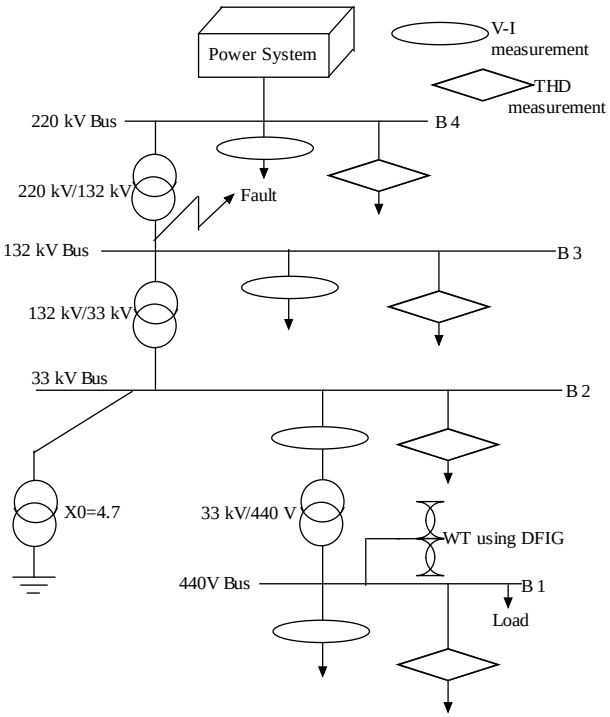

Fig. 1: Power System Model Integrated with Wind Power using DFIG

While modeling DFIG, the generator convention will be used, which means that the currents are outputs instead of inputs and real power and reactive power have a positive sign when they are fed into the grid. The d-q reference frame is rotating at synchronous speed with the q-axis 90° ahead of the d-axis. The position of the d-axis coincides with the maximum of the stator flux. The flux linkages can be calculated using the following set of equations in per unit :

$$\varphi_{ds} = -(L_s + L_m)\,i_{ds} - L_m \quad (9)$$

$$\varphi_{qs} = -(L_s + L_m)\,i_{qs} - L_m \quad (10)$$

ISBN: 978-960-474-370-4

$$\varphi_{dr} = -(L_r + L_m)\, i_{dr} - L_m \quad (11)$$

$$\varphi_{qr} = -(L_r + L_m)\, i_{qr} - L_m \quad (12)$$

where L_s and L_r are stator and rotor leakage inductance respectively and L_m is the mutual inductance between the stator and the rotor. The rotor slip s is defined as :

$$s = \frac{\omega_s - \frac{p}{2}\omega_m}{\omega_s} \quad (13)$$

where p is the number of poles and ω_m is the mechanical frequency of the generator. The active power P and reactive power Q generated by the DFIG :

$$P = v_{ds} i_{ds} + v_{qs} i_{qs} + v_{dr} i_{dr} + v_{qr} \quad (14)$$

$$Q = v_{qs} i_{ds} - v_{ds} i_{qs} + v_{qr} i_{dr} - v_{dr} \quad (15)$$

Equation 9 to Equation 15 describes the electrical part of a DFIG. However, also the mechanical part should be taken into account in developing a dynamic model. The following equation gives electromechanical torque T_e generated by DFIG :

$$T_e = \varphi_{dr}\, i_{qr} - \varphi_{qr} \quad (16)$$

The mechanical torque can be calculated by dividing power extracted from the wind, P_w by the mechanical generator frequency ω_m. The changes in generator speed that result from a difference in electrical and mechanical torque are calculated as :

$$\frac{d\omega}{dt} = \frac{1}{2H}\left(T_m - T_e\right) \quad (17)$$

where H is the inertia constant and T_m is the mechanical torque. The design parameters of DFIG are shown in Table 2.

Table 2: Design Parameters of DFIG

Generator Data for One Turbine	
Nominal Electrical Power	3.33 x 10^6 VA
Stator Resistance, R_s	0.023 p.u.
Stator Inductance, L_s	0.18 p.u.
Rotor Resistance, R_r	0.016 p.u.
Rotor Inductance, L_r	0.16 p.u.
Magnetizing Inductance, L_m	2.9 p.u.
Inertia Constant, H	0. 685
Pairs of Poles, p	3

The WECS considered for analysis consist of a DFIG driven by a wind turbine, rotor side converter and grid side converter, as shown in Fig.2.

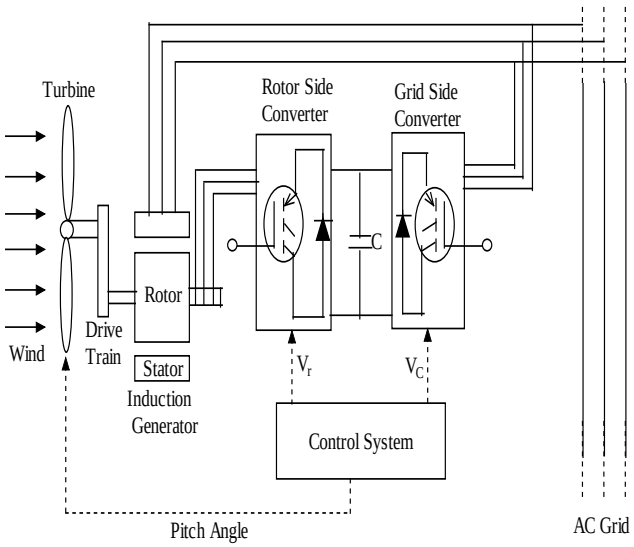

Fig.2: WECS with DFIG and Converters

Rotor side converter consists of three phase IGBT-Diode rectifier connected in Graetz bridge configuration with snubber resistance and capacitance. The power is controlled in order to follow a pre-defined power-speed characteristic, named tracking characteristic. The circuit is discretized at a sample time of 2 micro seconds. Grid side converter also consists of three phase IGBT-Diode rectifier connected in Graetz bridge configuration. The grid side converter is used to regulate the voltage of the DC bus capacitor.

The pitch angle control is used to limit the power extracted at high wind speeds conditions. In this model the wind speed is maintained constant at 10 m/sec. The control system uses a torque controller in order to maintain the speed. The reactive power produced by the wind turbine is also regulated at zero MVAR.

Rotor side converter consists of three-phase IGBT-diode rectifier connected in Graetz bridge configuration with snubber resistance and capacitance. The values of snubber resistance R_s and snubber capacitance C_s for rotor converter are derived from the following criteria:

- The snubber leakage current at fundamental frequency is less than 0.1% of nominal current when power electronic devices are not conducting.
- The time constant (RC) of snubbers is higher than 2 time sample time ($2\times T_s$).

The circuit is discretized at a sample time of 2 µs. Fig.3 shows voltage and VAR regulation of rotor

ISBN: 978-960-474-370-4

side converter. A Proportional-Integral (PI) regulator is used to reduce the power error to zero. The actual component of positive-sequence current (I_{qr}) is compared to I_{qr_ref} and the error is reduced to zero by a current regulator (PI). The output voltage of this regulator is q-axis rotor voltage V_{qr}. The reactive power at grid terminals is kept constant by a VAR regulator.

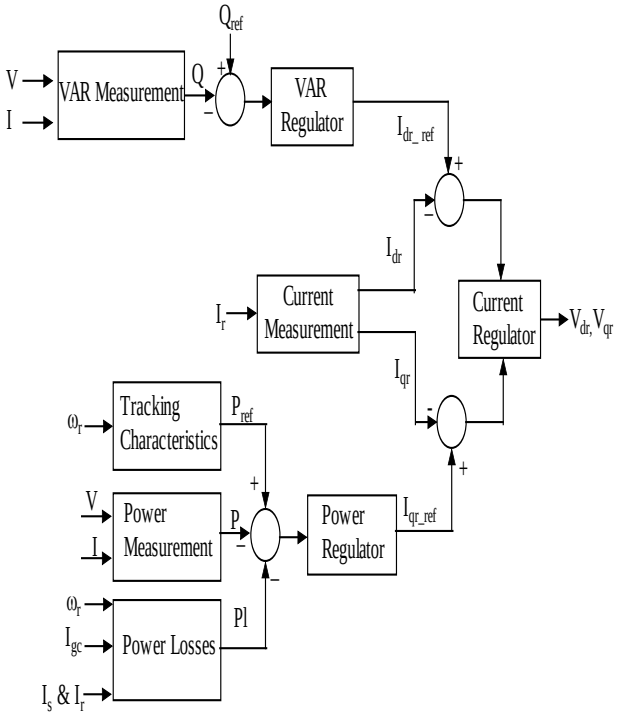

Fig.3: Regulators of Rotor Side Converter.

The output of the voltage regulator or VAR regulator is d-axis reference rotor current I_{dr_ref} which is injected in the rotor by rotor converter. The same current regulator is used to regulate the actual component of positive-sequence current (I_{dr}). The output of this regulator is the d-axis rotor voltage V_{dr}. The control system of grid side converter, illustrated in the Fig.4 consists of:

- Measurement systems which measure d-axis and q-axis components of AC positive-sequence currents to be controlled as well as the DC voltage V_{dc}.

- An outer regulation loop which consists of a DC voltage regulator. The output of the DC voltage regulator is the reference DC current I_{dc_ref} for the current regulator (I_{dc} = current in phase with grid voltage which controls active power flow).

- An inner current regulation loop which consists of a current regulator. The current regulator controls the magnitude and phase of the voltage generated by converter (V_c) from the I_{dc_ref} produced by the DC voltage regulator and specified I_{q_ref}.

The pitch angle is regulated at zero degree by pitch angle regulator until the speed w_r reaches desired speed of the tracking characteristic w_d. Beyond w_d, the pitch angle is proportional to the speed deviation from desired speed. The control system is illustrated in the Fig.5.

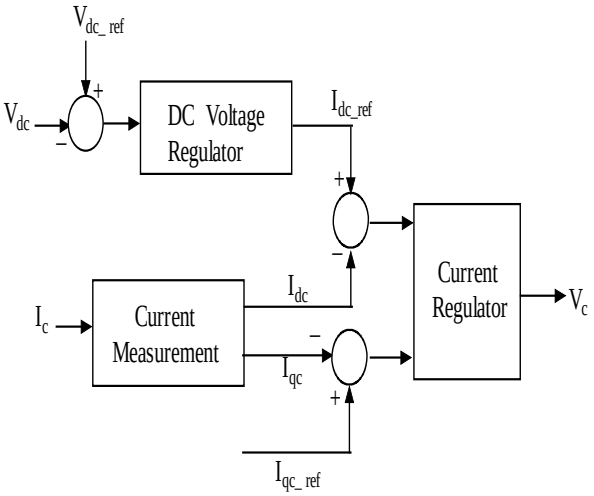

Fig.4: Regulators of Grid Side Converter

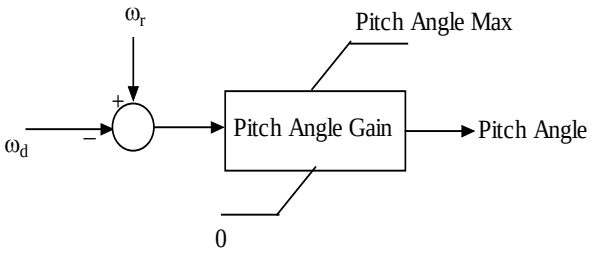

Fig.5: Pitch Control System.

4 Results and Discussions

THD measured at different buses during unsymmetrical and symmetrical faults and at different fault locations is shown in Table 3. It is observed that THD is maximum when measured at bus B1 during single phase fault at bus B1 and minimum when measured at bus B4 during phase to phase to ground fault at bus B1. THD values are compariteveley less when measured at bus B4 and more when measured at bus B1. It is observed that THD measured at bus B1 is same when fault occurs at bus B4 irrespective of type of fault. The same is true when THD is measured at buses B2 to B4. THD is more when measured at Bus B1, decreases as bus voltages increase, becoming minimum when measured at Bus B4.

ISBN: 978-960-474-370-4

Table 3: THD Measured at Different Buses

Fault Location	THD Measured (% of Fundamental) at Bus B1					
	1φ	1φG	2φ	2φG	3φ	3φG
Bus B1	9.94	9.4	7.68	7.79	6.39	6.69
Bus B2	9.8	8.96	7.68	7.68	7.42	7.42
Bus B3	10.52	9.76	7.94	8.9	9.76	7.24
Bus B4	9.89	9.89	9.89	9.89	9.89	9.89
Fault Location	THD Measured (% of Fundamental) at Bus B2					
	1φ	1φG	2φ	2φG	3φ	3φG
Bus B1	5.27	5.29	5.28	5.42	4.93	5.02
Bus B2	5.1	5.4	8.18	7.59	7.33	7.33
Bus B3	5.46	6.26	5.32	5.62	6.26	5.7
Bus B4	5.32	5.32	5.32	5.32	5.32	5.32
Fault Location	THD Measured (% of Fundamental) at Bus B3					
	1φ	1φG	2φ	2φG	3φ	3φG
Bus B1	2.31	2.34	2.94	3.03	3.39	3.36
Bus B2	2.19	2.72	7.68	7.45	7.31	7.31
Bus B3	2.8	4.08	3.79	4.1	4.06	4.51
Bus B4	2.29	2.29	2.29	2.29	2.29	2.29
Fault Location	THD Measured (% of Fundamental) at Bus B4					
	1φ	1φG	2φ	2φG	3φ	3φG
Bus B1	0.11	0.09	0.08	0.07	0.13	0.11
Bus B2	0.09	0.1	0.28	0.29	0.3	0.3
Bus B3	0.14	0.18	0.17	0.19	0.18	0.19
Bus B4	0.1	0.1	0.1	0.1	0.1	0.1

5 Conclusion

An attempt has been made in this paper to analyse the performances of the WECS based on DFIG, pertaining to power quality, active power, reactive power and speed control that each of the generators can handle. The system models are developed in the MATLAB/Simulink. This paper has presented the detailed model of the variable speed wind turbine with DFIG connected to power grid through back to back power electronic interface simulated. THD is measured at different locations during different faults at different buses. It is observed that THD is more when measured at Bus B1, decreases as bus voltages increase, becoming minimum when measured at Bus B4.

References:

[1] H Li, Z Chen, "Overview of Different Wind Generator Systems and their Comparisons", *IET Renewable Power Generation*, Vol. 2, No. 2, 2008, pp. 123-138.

[2] D. Rajib, VT Ranganathan, "Variable Speed Wind Power Generation using Doubly Fed Wound Rotor Induction Machine - A Comparison with Alternative Schemes," *IEEE Transactions on Energy conversion*, Vol. 17, No. 3, 2002, pp. 414-421.

[3] R. Mittal, KS Sandhu, DK. Jain, "An Overview of Some Important Issues Related to Wind Energy Conversion System (WECS)", *International Journal of Environmental Science and Development*, Vol. 1, No. 4, 2010, pp. 351-363.

[4] F.A. Ramirez, M.A. Arjona, "Development of a Grid-Connected Wind Generation System with a Modified PLL Structure", *IEEE Transactions on Sustainable Energy*, July 2012, Vol. 3, Issue 3, pp. 474 - 481.

[5] R.J. Wai, C.Y. Lin, Y.R. Chang, "Novel Maximum-Power-Extraction Algorithm for PMSG Wind Generation System", *IET Electric Power Applications*, Vol. 1, Issue 2, Mar. 2007, pp.275-283.

[6] Y.M. Kawale, S. Dutt, "Comparative Study of Converter Topologies used for PMSG Based Wind Power Generation", *Proc. Int. Conf. on Computer and Electrical Engg*., Dubai, Dec. 28-30, 2009, Vol. 2, pp. 367-371.

[7] B. Chitti, K.B. Mohanty, "Doubly Fed Induction Generator for Variable Speed Wind Energy Conversion Systems – Modeling and Simulation," *International Journal of Computer and Electrical Engineering*, Vol. 2, No. 1, 2010, pp. 141-147.

[8] LM Fernandez, CA Garcia, F Jurado, "Comparative Study on the Performance of Control Systems for DFIG Wind Turbines Operating with Power Regulation", *Energy 33*, 2008, pp. 1438-1452.

[9] J.G. Slootweg, H. Polinder, W.L. Kling, "Dynamic Modeling of a Wind Turbine with Doubly Fed Induction Generators", *IEEE Power Engg. Society Summer Meeting, Vancouver*, BC, Jul.15-19, Vol. 1, 2001, pp. 644-649.

[10] D. Liu, J. Hu, C. Zhang, "Blade Design for a Horizontal Axis Variable Speed Wind-Driven Generator", *World Non-Grid-Connected Wind Power and Energy Conf.*, Nanjing, Nov. 5-7, 2009, pp. 1-4.